CrossMark

INTEGRAL Limits on Past High-energy Activity from FRB 20200120E in M81

S. Mereghetti[1] , M. Topinka[1,2], M. Rigoselli[1] , and D. Götz[3]

[1] INAF—Istituto di Astrofisica Spaziale e Fisica Cosmica, Via A. Corti 12, I-20133 Milano, Italy
[2] Department of Theoretical Physics and Astrophysics, Faculty of Science, Masaryk University, Kotlářská 2, Brno 611 37, Czech Republic
[3] AIM-CEA/DRF/Irfu/Département d'Astrophysique, CNRS, Université Paris-Saclay, Université de Paris, Orme des Merisiers, F-91191 Gif-sur-Yvette, France

Abstract

The repeating fast radio burst FRB 20200120E is located in a globular cluster belonging to the nearby M81 galaxy. Its small distance (3.6 Mpc) and accurate localization make it an interesting target to search for bursting activity at high energies. From 2003 November to 2021 September, the INTEGRAL satellite has obtained an exposure time of of 18 Ms on the M81 sky region. We used these data to search for hard X-ray bursts from FRB 20200120E using the IBIS/ISGRI instrument, without finding any significant candidate, down to an average fluence limit of $\sim 10^{-8}$ erg cm^{-2} (20–200 keV). The corresponding limit on the isotropic luminosity for a burst of duration Δt is $\sim 10^{45} \left(\frac{10 \, \text{ms}}{\Delta t} \right)$ erg s^{-1}, the deepest limit obtained for an extragalactic FRB in the hard X-ray range. This rules out the emission of powerful flares at a rate higher than 0.1 yr^{-1} that could be expected in models invoking young hyperactive magnetars.

Unified Astronomy Thesaurus concepts: Magnetars (992); Radio bursts (1339)

1. Introduction

The discovery of an extremely bright and short radio burst from the Galactic soft gamma-ray repeater SGR 1935+2154 on 2020 April 28 (CHIME/FRB Collaboration et al. 2020; Bochenek et al. 2020), provided strong observational support to the connection between fast radio bursts (FRBs) and magnetars. FRBs are short ($\sim$ms) and bright pulses of coherent radio emission with high dispersion measure, implying an extragalactic origin (see Petroff et al. 2019; Cordes & Chatterjee 2019 for reviews), while magnetars are isolated neutron stars powered by magnetic energy (see Mereghetti et al. 2015; Turolla et al. 2015; Kaspi & Beloborodov 2017 for reviews). A connection with magnetars had been postulated in several of the FRB models, involving emission either in the star magnetosphere or in relativistically ejected material (see, e.g., Zhang 2020 and references therein).

The bright FRB-like radio burst of 2020 April 28 from SGR 1935+2154 was accompanied by the simultaneous emission of hard X-rays with properties similar to those of the short bursts (duration <1 s, peak luminosity $\sim 10^{39-41}$ erg s^{-1}) typical of SGR 1935+2154 and other Galactic magnetars, except for a harder spectrum (Mereghetti et al. 2020; Li et al. 2021; Ridnaia et al. 2021). The ratio between the radio and X-ray fluences of the 2020 April 28 burst was $\eta \sim 3 \times 10^{-5}$. Fainter radio bursts subsequently observed from SGR 1935+2154 were not seen at high energies (Kirsten et al. 2021a), consistent with similar values of η. On the other hand, the lack of a radio burst associated with the 2004 December 27 giant flare of SGR 1806–20 (Palmer et al. 2005) implies $\eta < 10^{-10}$ (Tendulkar et al. 2016), indicating that the ratio of radio to high-energy fluence in magnetar bursts can span a wide range of values.

Searches for X-ray counterparts of FRBs, already carried out in the past without success (Scholz et al. 2017; Cunningham et al. 2019; Guidorzi et al. 2019; Martone et al. 2019), received renewed interest after the SGR 1935+2154 results. However, the extragalactic distances of FRBs result in much lower fluxes compared to those of galactic magnetars (SGR 1935+2154 has a distance of $4.4^{+2.8}_{-1.3}$ kpc; Mereghetti et al. 2020). Up to now, only upper limits have been reported for their high-energy emission (Guidorzi et al. 2020; Pilia et al. 2020; Scholz et al. 2020; Verrecchia et al. 2021).

Recently, the repeating FRB 20200120E has been discovered in the outskirts of the spiral galaxy M81 (Bhardwaj et al. 2021a). Its association with this nearby galaxy, already suggested by the FRB dispersion measure of only 88 pc cm^{-3}, has been confirmed by a subarcsecond localization that shows positional coincidence with a globular cluster belonging to M81 (Kirsten et al. 2021b). With a distance of only 3.6 Mpc, FRB 20200120E is by far the closest extragalactic FRB. Therefore, also considering its repeating nature, it is a very interesting target for multiwavelength observations. These observations allow us to sample luminosities $\sim$2000 times below the limits obtained for FRB 20180916B, which is the next closest repeating FRB with an identified host galaxy (d $\sim$ 150 Mpc; Marcote et al. 2020). We note that another interesting target in this respect is FRB 20181030A, if its recently suggested association with NGC 3252 at $\sim$20 Mpc (Bhardwaj et al. 2021b) is confirmed. A search for persistent X-ray sources at the position of FRB 20200120E was done with Chandra by Kirsten et al. (2021b), who obtained a luminosity upper limit of 2×10^{37} erg s^{-1} (0.5–10 keV). They also noticed the lack of γ-ray sources in the Fermi/LAT catalogs at the M81 position.

Here we report on a search for hard X-ray bursts from FRB 20200120E carried out using the archival data of the INTEGRAL satellite, which collected an exposure time of 18 million seconds on M81 from 2003 November to 2021 September.

2. Data Analysis and Results

Our results are based on data collected by the Imager on-board INTEGRAL (IBIS; Ubertini et al. 2003). IBIS is a coded mask instrument providing images with angular resolution of $\sim$12′ over a total field of view of 29° × 29°. In particular, we used the data obtained with ISGRI (INTEGRAL Soft Gamma Ray Imager; Lebrun et al. 2003), the lower energy detector of

Table 1
Observation Log

Revolutions	Start Date	End Date	Off-axis Angles	Net Exposure Fully coded FoV	Net Exposure Total
			(degrees)	(ks)	(ks)
132-133	2003-11-12	2003-11-17	9.3–15.6	0	197
179-180	2004-04-02	2004-04-06	9.0–16.3	0	141
221-224	2004-08-04	2004-08-14	11.8–13.8	0	92
250	2004-10-30	2004-10-31	7.9–8.0	0	4
669	2008-04-07	2008-04-07	16.7–16.7	0	1
856-872	2009-10-17	2009-12-06	0.3–8.1	1077	1626
930-933	2010-05-28	2010-06-05	0.5–9.8	154	241
960-962	2010-08-24	2010-08-31	13.3–15.1	0	10
971-977	2010-09-26	2010-10-16	0.9–15.0	73	108
1029-1051	2011-03-18	2011-05-24	0.4–8.3	602	883
1092-1096	2011-09-24	2011-10-06	1.6–7.9	39	61
1111-1115	2011-11-20	2011-12-02	0.6–8.0	316	495
1156	2012-04-03	2012-04-03	8.0–8.1	0	5
1173	2012-05-22	2012-05-22	14.4–14.7	0	2
1216-1254	2012-09-30	2013-01-20	0.3–8.1	1107	1681
1347-1364	2013-10-25	2013-12-16	0.3–20.5	1179	2162
1380-1407	2014-01-31	2014-04-24	0.0–9.6	2916	4512
1419-1432	2014-05-27	2014-07-08	0.1–8.2	1432	2154
1524	2015-03-30	2015-03-30	7.9–8.0	0	8
1558-1564	2015-06-30	2015-07-16	10.5–10.7	0	3
1652	2016-03-05	2016-03-05	8.1–8.2	0	6
1671-1681	2016-04-25	2016-05-22	11.5–16.0	0	282
1852	2017-08-20	2017-08-20	2.9–3.9	1	1
1873-1874	2017-10-15	2017-10-18	3.9–4.0	3	3
2117-2119	2019-07-26	2019-07-29	14.3–14.9	0	11
2151-2167	2019-10-24	2019-12-04	0.5–13.5	808	1204
2227-2228	2020-05-13	2020-05-16	1.2–8.0	102	151
2278-2307	2020-09-24	2020-12-11	0.7–8.1	502	727
2334-2372	2021-02-21	2021-06-03	0.4–17.7	785	1149
2395-2410	2021-08-02	2021-09-11	0.3–6.9	100	150
TOTAL				11196	18067

IBIS, which operates in the nominal 15–1000 keV range and provides photon-by-photon events tagged with a time resolution of 61 μs. The ISGRI detection plane consists of 128×128 pixels, grouped into eight modules, giving a total sensitive area of 2600 cm^2 on-axis. For sources located in the central $9° \times 9°$ of the field of view (FoV), the whole detector area receives flux modulated by the coded mask. In this region (the fully coded FoV) the sensitivity is highest and nearly uniform. For sources at larger off-axis angles (the partially coded FoV) only a fraction of the detection plane receives the flux modulated by the coded mask, and thus the sensitivity gradually decreases.

The position of FRB 20200120E has been repeatedly observed by INTEGRAL, with long campaigns dedicated to M81 (Mereminskiy et al. 2016), as well as serendipitously, during observations of other nearby targets. Due to the dithering observing mode used by INTEGRAL, the data are split into many short pointings with typical duration between 30 and 60 minutes each, called science windows (ScWs). We selected for our analysis all the ScWs that contain the position of FRB 20200120E, including those in which it was located at large off-axis angles. The data were retrieved from the local archive of public INTEGRAL data maintained at IASF-Milano (Paizis et al. 2013). Our search consisted of two main steps: the first one, based only on the timing analysis of the ISGRI light curves, aimed at finding burst candidates; the second step was an imaging analysis of the candidates, aimed at understanding their

nature and possibly associating them with FRB 20200120E or other sources in the instrument FoV.

To increase the signal-to-noise ratio, all the light curves were extracted using only the ISGRI pixels with a source illumination fraction greater than 0.5. For most of the time, the instrumental background induced by cosmic rays, as well as that caused by bright X-ray sources inside (or close to) the FoV, vary on timescales longer than the ScW duration. ScWs with particularly high and variable background typically occur when INTEGRAL is close to the Earth's radiation belts, at the beginning or at the end of the satellite revolutions,[4] or during periods of intense solar activity. Such ScWs were excluded from our search, resulting in the net exposure times reported in Table 1.

For each ScW, we determined the background by fitting a constant to the light curve of the whole detector binned at one second, after correcting for time intervals in which one or more ISGRI modules were not operating[5] and iteratively removing the bins more than three standard deviations above the average. Such "3σ clipping" is done to have a better estimate of the background level during the "quiet" part of the ScW. Inclusion of bright bins (often caused by bursts from sources outside the

---

[4] INTEGRAL is on a highly elliptical orbit with a period of 3 days until 2015 January and 2.7 days afterward.
[5] Modules with too many noisy pixels are temporarily switched off by the on-board software.
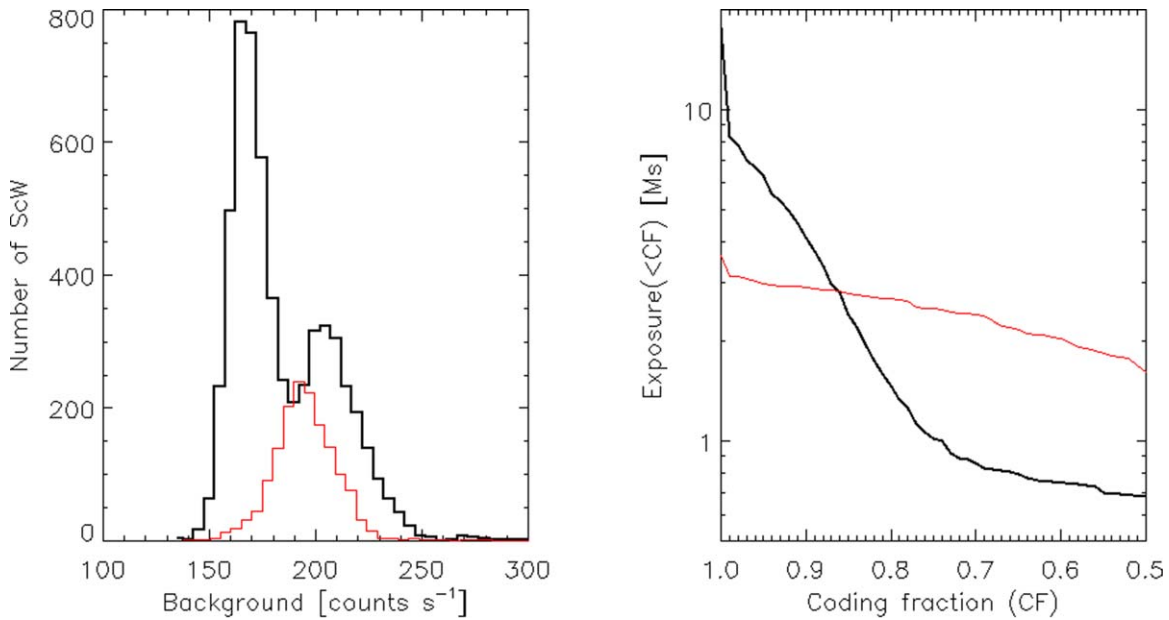
Figure 1. Left: distribution of background count rates (20–200 keV) of the ScW used in the search for bursts from FRB 20200120E (black) and in the observations of SGR 1806–20 used for comparison (red). The count rates have been corrected for the coding fraction (i.e., the fraction of detector area over which the photons coming from the source direction are modulated by the coded mask aperture pattern). Right: distribution of net exposure time as a function of coding fraction for FRB 20200120E (black) and for SGR 1806–20 (red).

field of view) would lead to an increased threshold level, thus reducing the sensitivity. Note that the time intervals with high count rate are removed only in the background computation, while they are kept for the following burst search.

We then searched for excesses above the expected background counts using sliding time windows with eight durations logarithmically spaced between 0.01 and 1.28 s. These are the typical durations of bursts from magnetars. Longer events would trigger on several adjacent bins, unless they have a very slow rise time (which would be atypical for a magnetar burst). Events shorter than 0.01 s and with a sufficiently high number of counts to be detected also in the images (∼30–100, depending on the position in the FoV) trigger also on the longer timescales. The thresholds were set to values corresponding to an expectation of ∼0.001 false positives per ScW and timescale. The search was done in two energy ranges: 20–200 keV and 20–100 keV. Excesses found in adjacent time bins and/or in overlapping timescales were grouped and considered as a single burst candidate for further imaging analysis.

The candidates found in the light curves were examined with the imaging software developed for the INTEGRAL Burst Alert System (IBAS; Mereghetti et al. 2003) as well as with a maximum likelihood method that exploits the knowledge of the source position in the field of view. Briefly, this consists of finding the source and background fluxes, which maximize the probability of obtaining the observed distribution of detector counts as a function of the pixel illumination fraction. The time integration for these analyses was optimized for each candidate by selecting only the time intervals with a number of counts above three standard deviations from the average in the light curves. None of the candidates could be confirmed as a burst positionally coincident with FRB 20200120E. The only candidate producing a source significantly detected in the images was GRB 121212A (Grupe et al. 2012). This burst, at angular distance of 12° from FRB 20200120E and at off-axis

angle of 6°, had previously been detected in real time as a subthreshold IBAS trigger (Higgins et al. 2017).

Although the faintest candidates had a number of counts below that required for imaging analysis, more than 200 of them were bright enough and should have produced a clearly detectable source, if originating from directions within the FoV. The most likely explanations for these events is that they were due to either background fluctuations or bursts from sources at large off-axis angles, outside the imaging FoV. In fact, the passive shielding that connects ISGRI to the coded mask becomes progressively transparent with increasing photon energy. In a few cases we could associate the events with GRBs seen by other satellites, based on their temporal coincidence. Two such examples are GRB 121118B (Hurley et al. 2012) and GRB 140306A (Golenetskii et al. 2014), which occurred at off-axis angles of 73° and 50°, respectively.

Several factors concur to determine the sensitivity of our search: the most relevant one is the FRB position in the FoV, which determines the detecor area collecting coded source photons. Other factors are the background rate and the secular increase in the low-energy threshold caused by the detector ageing. Finally, the spectral shape, duration, and time profile of the burst also have an effect on the sensitivity, but these properties do not vary much for the typical magnetar bursts. The distribution of the background count rates in the ScWs used in our search (left panel of Figure 1) has two peaks, at ∼170 and ∼200 counts s^{-1}. On long timescales, the background variations follow the 11 yr cycle of solar activity. The background is higher at the minimum of solar activity. The bimodal shape of the distribution shown in the figure reflects how the ScWs were distributed in time. As can be seen in Table 1 and Figure 1 (right panel), FRB 20200120E was observed at small off-axis angles for most of the time: only for ∼1 (0.7) Ms it was at positions with coding fractions below 0.75 (0.5), where the sensitivity is <85% (75%) of the optimal on-axis value. It is thus clear from the distributions of Figure 1 that the ScWs used in our search had different sensitivities.
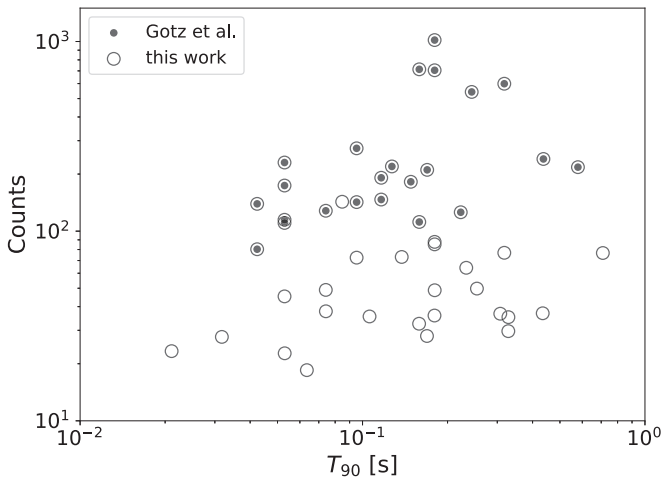
Figure 2. The circles show the number of counts and duration of the bursts from SGR 1806–20 detected during revolutions 108-122 (from 2003 September 1 to October 15). The dots mark the bursts also detected by Götz et al. (2004b).

To test our burst search procedure and to estimate its sensitivity, we applied it to the ISGRI data obtained in 2003–2004 for the magnetar SGR 1806−20, during a period of bursting activity (Götz et al. 2004a, 2006). Compared to the M81 data, these observations include a higher fraction of ScWs with the source at large off-axis angles and, due to the presence of the Galactic ridge diffuse emission, their background rate is generally higher than that of the M81 data taken at the same phase of the 11 yr solar cycle. As shown by the red histogram in Figure 1, most of the M81 ScW had a background rate similar or lower than that of the SGR 1806−20 data used for comparison (red histogram in Figure 1). Therefore, using these SGR 1806−20 data we obtain a conservative estimate of the average sensitivity reached in our search.

We detected from SGR 1806–20 almost twice as many bursts that had been reported by these authors. As an example, we show in Figure 2 the results for the time period from 2003 September 1 to October 15, that can be directly compared to those of Götz et al. (2004b). Our search algorithm is able to reveal fainter bursts because the previous works were based on the triggers found during the IBAS real time analysis. IBAS monitors the overall count rate of the whole detector, without exploiting the a priori knowledge of the source position to optimize the light curve extraction (as instead we do in this work). Götz et al. (2006), assuming a thermal bremsstrahlung spectrum with temperature $kT = 32$ keV, measured a 15–100 keV fluence of $\sim 10^{-8}$ erg cm^{-2} for their faintest bursts. Converting to the 20–200 keV range and considering kT in the 20–70 keV range would change this value by less than 30%. Therefore, although we could also reveal fainter bursts from SGR 1806–20 and the data on M81 had more favorable background and coding fraction conditions, we conservatively take 10^{-8} erg cm^{-2} (20–200 keV) as a representative fluence upper limit valid for the bulk of the FRB 20200120E observations reported here.

3. Discussion

We carried out a search for hard X-ray (>20 keV) bursts from the direction of FRB 20200120E in 18 Ms of INTEGRAL data without finding any significant candidate. This nondetection rules out the emission of bursts with fluence above $\sim 10^{-8}$ erg cm^{-2} during most of our observations. At the distance of 3.6 Mpc, implied by the location of FRB 20200120E in the

core of a globular cluster of M81, this corresponds to a limit on the isotropic equivalent energy of $\sim 10^{43}$ erg, the deepest limit obtained for an FRB in the hard X-ray range. The bursts from FRB 20200120E observed at 400–800 MHz with CHIME in 2020 (Bhardwaj et al. 2021a) and the one of 2021 March 2 seen at 2.25 GHz (Majid et al. 2021), with isotropic radio energies of $\sim (1 - 2) \times 10^{34}$ erg, are the most energetic ones seen from this repeater. Other less energetic bursts were seen at 1.4 GHz (Nimmo et al. 2021). Unfortunately, the time intervals of our search do not include any of these bursts. If bursts of similar radio energy occurred during the INTEGRAL observations analyzed here, our limit would imply a ratio of radio to X-ray fluence $\eta \gtrsim 10^{-9}$.

Our limit cannot rule out short SGR-like bursts from FRB 20200120E. The energy emitted in typical magnetar bursts, with durations shorter than one second, rarely exceeds a few 10^{41} erg (Israel et al. 2008; van der Horst et al. 2012; Lin et al. 2020; Younes et al. 2020). The 2020 April 28 burst from SGR 1935+2154 had a hard X-ray energy of $\sim 3 \times 10^{39} \left(\frac{d}{5 \, kpc} \right)^2$ erg and $\eta \sim 3 \times 10^{-5}$ (Mereghetti et al. 2020; Ridnaia et al. 2021). On the other hand, the three giant flares observed from SGR 0526–66, SGR 1900+14, and SGR 1806–20 emitted 10^{44-46} erg in their short (<0.4 s) initial spikes (Mazets et al. 1999; Hurley et al. 2005). Similar events at the distance of M81 would have been clearly detected in our search.[6] We note, however, that the net exposure time of about half a year obtained for FRB 20200120E with INTEGRAL in 18 yr, is relatively small if one considers that only three giant flares have been detected from the Galactic magnetars observed (although with discontinuous monitoring) for ~ 40 yr.

The lack of bursts from FRB 20200120E in the INTEGRAL data is constraining in the context of models involving young and very active magnetars. Several FRB models invoke the presence of magnetars with ages below a few tens of years, much younger than those observed in our Galaxy (Metzger et al. 2017; Beloborodov 2020; Lu et al. 2020; Dall'Osso & Stella 2021). The latter have estimated ages of several tens of kiloyears or longer, although some possibly younger magnetars have been recently found (Esposito et al. 2020). Young and rapidly spinning magnetars are believed to emit bursts and flares more frequently and with higher energy than the older known magnetars. In fact, the activity level, as measured by the frequency and energetics of bursts and outbursts, declines with time, as the very large initial rotational energy decreases and the magnetic field stored in the star dissipates (Perna & Pons 2011; Dehman et al. 2020). The probability of observing zero bursts in 0.5 yr of data is $e^{-R/2}$, where R is the burst rate per year. Our null results imply $R < 0.1$ yr^{-1} (at 95% c.l.) for bursts with luminosity above $\sim 10^{45} \left(\frac{10 \, ms}{\Delta t} \right)$ erg s^{-1}, where Δt is the burst duration.

We finally note that the location in a globular cluster with estimated age of ~ 10 Gyr (Kirsten et al. 2021b) makes it unlikely that FRB 20200120E was born in the collapse of a massive star, the favorite channel proposed for the formation of magnetars. Possible alternative origins are the merging of two compact objects (neutron stars and/or white dwarfs) or the accretion induced collapse of a white dwarf. These evolutionary channels

---

[6] Bhardwaj et al. (2021a) noticed that the burst of 2020 July 18 was in the FoV of Swift/BAT and the candidate burst of 2020 February 6 was visible by Fermi/GBM, but no detections with these instruments were reported. The estimated limits rule out a magnetar giant flare emission associated with these two events.

involve binary systems and are favored by the high stellar density found in the cores of globular clusters. However, the implied birth rates are relatively small thus requiring that FRB like the one in M81 must have active lifetimes larger than 10^4 yr (Kremer et al. 2021; Lu et al. 2021). The lack of strong bursting activity from FRB 20200120E in the INTEGRAL data is consistent with this scenario and supports the view that not all FRBs are related to young hyperactive magnetars.

4. Conclusions

Our extensive search for hard X-ray magnetar-like bursts from FRB 20200120E in the INTEGRAL/IBIS data obtained from 2003 November to 2021 September did not reveal any significant event at the position of this repeating FRB. Being associated with a globular cluster in M81, FRB 20200120E is by far the closest among the well localized FRBs. Given its distance of 3.6 Mpc, the average sensitivity of our search corresponds to limits of $\sim10^{43}$ erg on the isotropic energy and $\sim10^{45}\left(\frac{10\,\mathrm{ms}}{\Delta t}\right)$ erg s^{-1} on the 20–200 keV luminosity, where Δt is the burst duration. We can thus exclude the emission of giant flares during the time periods in which FRB 20200120E was in the IBIS field of view (~18 Ms, in total). This supports the idea that FRB 20200120E is not a young hyperactive magnetar, as also suggested by its lower luminosity and location in a globular cluster.

Although FRB 20200120E might not be representative of the bulk of the FRB population, it is a very interesting target for multiwavelength campaigns. Coordinated radio and high-energy observations of this source, and other FRBs possibly associated with nearby galaxies (e.g., FRB 20181030A; Bhardwaj et al. 2021b), can significantly constrain models for the emission of radio bursts and possibly lead to the discovery of the first bursts from an extragalactic FRB.Acknowledgments

ORCID iDs

S. Mereghetti ● https://orcid.org/0000-0003-3259-7801
M. Rigoselli ● https://orcid.org/0000-0001-6641-5450
D. Götz ● https://orcid.org/0000-0001-9494-0981

References

Beloborodov, A. M. 2020, ApJ, 896, 142
Bhardwaj, M., Gaensler, B. M., Kaspi, V. M., et al. 2021a, ApJL, 910, L18
Bhardwaj, M., Kirichenko, A. Y., Michilli, D., et al. 2021b, ApJ, 919, L24
Bochenek, C. D., Ravi, V., Belov, K. V., et al. 2020, Natur, 587, 59
CHIME/FRB Collaboration, Andersen, B. C., Bandura, K. M., et al. 2020, Natur, 587, 54
Cordes, J. M., & Chatterjee, S. 2019, ARA&A, 57, 417
Cunningham, V., Cenko, S. B., Burns, E., et al. 2019, ApJ, 879, 40
Dall'Osso, S., & Stella, L. 2021, arXiv:2103.10878
Dehman, C., Viganò, D., Rea, N., et al. 2020, ApJL, 902, L32
Esposito, P., Rea, N., Borghese, A., et al. 2020, ApJL, 896, L30
Golenetskii, S., Aptekar, R., Pal'Shin, V., et al. 2014, GCN, 15938, 1
Götz, D., Mereghetti, S., Mirabel, I. F., & Hurley, K. 2004a, A&A, 417, L45
Götz, D., Mereghetti, S., Mirabel, I. F., et al. 2004b, in ESA Spec. Publ. 552, 5th INTEGRAL Workshop on the INTEGRAL Universe, ESA SP-552, ed. V. Schoenfelder, G. Lichti, & C. Winkler (Noordwijk: ESA), 615
Götz, D., Mereghetti, S., Molkov, S., et al. 2006, A&A, 445, 313
Grupe, D., Baumgartner, W. H., Guidorzi, C., et al. 2012, GCN, 14064, 1
Guidorzi, C., Marongiu, M., Martone, R., et al. 2019, ApJ, 882, 100
Guidorzi, C., Marongiu, M., Martone, R., et al. 2020, A&A, 637, A69
Higgins, A. B., Starling, R. L. C., Götz, D., et al. 2017, MNRAS, 470, 314
Hurley, K., Boggs, S. E., Smith, D. M., et al. 2005, Natur, 434, 1098
Hurley, K., Mitrofanov, I. G., Golovin, D., et al. 2012, GCN, 13977, 1
Israel, G. L., Romano, P., Mangano, V., et al. 2008, ApJ, 685, 1114
Kaspi, V. M., & Beloborodov, A. M. 2017, ARA&A, 55, 261
Kirsten, F., Marcote, B., Nimmo, K., et al. 2021b, arXiv:2105.11445
Kirsten, F., Snelders, M. P., Jenkins, M., et al. 2021a, NatAs, 5, 414
Kremer, K., Piro, A. L., & Li, D. 2021, ApJL, 917, L11
Lebrun, F., Leray, J. P., Lavocat, P., et al. 2003, A&A, 411, L141
Li, C. K., Lin, L., Xiong, S. L., et al. 2021, NatAs, 5, 378
Lin, L., Göğüş, E., Roberts, O. J., et al. 2020, ApJ, 893, 156
Lu, W., Beniamini, P., & Kumar, P. 2021, arXiv:2107.04059
Lu, W., Kumar, P., & Zhang, B. 2020, MNRAS, 498, 1397
Majid, W. A., Pearlman, A. B., Prince, T. A., et al. 2021, ApJL, 919, L6
Marcote, B., Nimmo, K., Hessels, J. W. T., et al. 2020, Natur, 577, 190
Martone, R., Guidorzi, C., Margutti, R., et al. 2019, A&A, 631, A62
Mazets, E. P., Cline, T. L., Aptekar, R. L., et al. 1999, AstL, 25, 635
Mereghetti, S., Götz, D., Borkowski, J., Walter, R., & Pedersen, H. 2003, A&A, 411, L291
Mereghetti, S., Pons, J. A., & Melatos, A. 2015, SSRv, 191, 315
Mereghetti, S., Savchenko, V., Ferrigno, C., et al. 2020, ApJL, 898, L29
Mereminskiy, I. A., Krivonos, R. A., Lutovinov, A. A., et al. 2016, MNRAS, 459, 140
Metzger, B. D., Berger, E., & Margalit, B. 2017, ApJ, 841, 14
Nimmo, K., Hessels, J. W. T., Kirsten, F., et al. 2021, arXiv:2105.11446
Paizis, A., Mereghetti, S., Götz, D., et al. 2013, A&C, 1, 33
Palmer, D. M., Barthelmy, S., Gehrels, N., et al. 2005, Natur, 434, 1107
Perna, R., & Pons, J. A. 2011, ApJL, 727, L51
Petroff, E., Hessels, J. W. T., & Lorimer, D. R. 2019, A&ARv, 27, 4
Pilia, M., Burgay, M., Possenti, A., et al. 2020, ApJL, 896, L40
Ridnaia, A., Svinkin, D., Frederiks, D., et al. 2021, NatAs, 5, 372
Scholz, P., Bogdanov, S., Hessels, J. W. T., et al. 2017, ApJ, 846, 80
Scholz, P., Cook, A., Cruces, M., et al. 2020, ApJ, 901, 165
Tendulkar, S. P., Kaspi, V. M., & Patel, C. 2016, ApJ, 827, 59
Turolla, R., Zane, S., & Watts, A. L. 2015, RPPh, 78, 116901
Ubertini, P., Lebrun, F., Di Cocco, G., et al. 2003, A&A, 411, L131
van der Horst, A. J., Kouveliotou, C., Gorgone, N. M., et al. 2012, ApJ, 749, 122
Verrecchia, F., Casentini, C., Tavani, M., et al. 2021, ApJ, 915, 102
Younes, G., Güver, T., Kouveliotou, C., et al. 2020, ApJL, 904, L21
Zhang, B. 2020, Natur, 587, 45